



# Characterization of magnetic iron phases in IMPACTITES by MÖSSBAUER spectroscopy

María L. Cerón Loayza<sup>1</sup>  · Jorge A. Bravo Cabrejo<sup>1</sup>

Published online: 20 August 2019  
© Springer Nature Switzerland AG 2019

## Abstract

We present the results for two mineral samples from the Natural History Museum (MHN) of San Marcos National University (UNMSM) classified as: potential meteoritic samples coded MHN08 and MHN09 with an iron content of about 10% that were characterized using physical techniques such as energy dispersive X-ray fluorescence (EDXRF), X-ray diffractometry (XRD) and transmission Mössbauer spectroscopy (TMS). This study reveals that the samples consist mainly of quartz, goethite and impactites such as coesite, stishovite, and ringwoodite, and therefore should be classified as impactites. <sup>57</sup>Fe Mössbauer spectroscopy allowed the observation of three subspectra, two of them assigned to magnetic iron phases, and a third subspectrum assigned to a superparamagnetic phase. An important contribution of TMS is the possibility of observing this superparamagnetic phase which is assigned to goethite which at RT shows a very broad area (80.8%), and at liquid helium temperature appears as a magnetically ordered sextet.

**Keywords** Mossbauer spectroscopy · Impactites · Magnetic iron phases

## 1 Introduction

In an interplanetary scheme of the world that surrounds us there are vestiges of planetary rocks, such as the meteorites that travel through the terrestrial atmosphere and impact the surface of our planet generating pressures and temperatures much greater than those generated by normal terrestrial metamorphism. This produces phase transformations in rocks named impactites.

---

This article is part of the Topical Collection on *Proceedings of the 16th Latin American Conference on the Applications of the Mössbauer Effect (LACAME 2018), 18-23 November 2018, Santiago de Chile, Chile*  
Edited by Carmen Pizarro Arriagada

---

✉ María L. Cerón Loayza  
mceronl@unmsm.edu.pe

<sup>1</sup> Laboratorio de Análisis de Suelos, Facultad de Ciencias Físicas, Universidad Nacional Mayor de San Marcos, Ap. Postal 14-0149, 14 Lima, Peru

Therefore, these are valuable witnesses that allow us to verify the occurrence of a meteoritic impact in a zone under surveillance.

This hypothesis motivated an interest in collecting mineral samples with an iron content of about 10% from the Natural History Museum (MHN) of San Marcos National University (UNMSM); Thus we requested the MHN of UNMSM to grant us access to some of their samples for study, thus obtaining eight samples to analyze, of which two were selected on the basis of their iron content and were coded as: MHN08 and MHN09.

Earlier undertaken studies had allowed us to observe and obtain results valuable about meteoritic samples as well as about the impactites themselves [1–3].

Figure 1 shows the graph: shock pressure (GPa) vs temperature (°C) reached in quartz, where phase transformations are depicted that take place in terrestrial surface rocks when impacted by a meteorite and very high pressures and temperatures are reached. Since quartz is the primary mineral whose elemental and structural composition are very hard to change, it is taken as a reference for the mineral polymorphs that can occur. Among them we have the well known coesite, stishovite and moldavite. At the high pressures that can derive from a meteoritic impact two types of collision metamorphosis can take place:

- 1) Phase changes and
- 2) Structural changes.

## 2 Materials and methods

The studied samples are shown in Fig. 2. They were selected due to their relatively high iron content. Sample MHN-08 had a mass of 12.90 g, and sample MHN-09 had a mass of 19.0 g; both samples were collected from Yagapasa Ladera – Rondobamba site, in the Huanuco Region, Peru.

These samples were characterized using the following physical techniques: energy dispersive X-ray fluorescence (EDXRF), X-ray diffractometry (XRD), transmission Mössbauer spectroscopy (TMS) and metallographic optical microscopy (MOM). TMS analysis was performed at room (RT) and liquid helium (LHT) temperatures. The Mössbauer spectra were fitted using the NORMOS program (Brand, 1995) in its site (SITE) and distribution (DIST) versions.

### 2.1 Analysis by energy dispersive X-ray fluorescence (EDXRF)

The elemental composition analysis was performed with a portable EDXRFAMPTTEK instrument. This instrument uses an X-ray tube with a Ag anode operating at 30 kV and 30  $\mu$ A. This instrument allows the identification and quantification of elements with  $Z > 13$  (aluminum). Results of these quantitative analyses are given in Table 1. This was done by fitting the experimental EDXRF spectrum using a program that simulates EDXRF spectra based on the fundamental parameters model; this program is written in FORTRAN and simulates all the physical processes that affect an X-ray spectrum: energy distribution of the primary and secondary X-rays, radiation propagation, scattering, absorption and photoelectric production, which take place in an EDXRF measurement taking into account the geometry of the experimental arrangement. It is based on data of X-ray cross sections provided by NIST and atomic characteristic X-ray parameters provided by IAEA. The X-ray distribution function, which includes continuous and

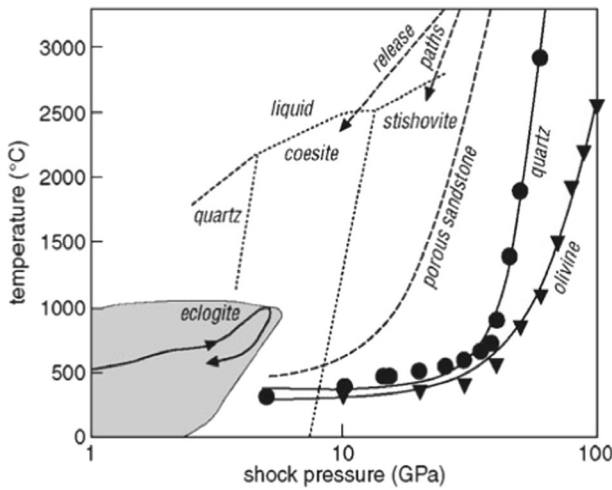


**Fig. 1** Phase diagram depicting the pressure temperature conditions reached in quartz, olivine (solid line), and porous sandstone (long dashed line) by shock compression (data after Wackerle [4], Kieffer et al. [5], Holland and Ahrens [6]). The release paths hold for porous quartz, which first melts on loading and then solidifies on cooling as coesite or stishovite. The equilibrium phase boundaries between quartz, coesite, stishovite and liquid are drawn as dashedlines



**Fig. 2** Photographs of the studied samples from the Natural History Museum

discrete components, has been calibrated by performing scattering of these primary X-rays by known samples. The performance of the program has been checked using reference samples. The estimated uncertainty in these measurements of the elemental concentrations is about 10%, depending on the atomic number of the element (Dr. J.A. Bravo C., private communication).

**2.2 Analysis by X-ray Diffractometry (XRD)**

For the structural analysis of the minerals present in the samples, the XRD technique was applied using a BRUKER diffractometer, model D8-Focus, with  $CuK\alpha$  (1.5406 Å) radiation (40 kV, 40 mA) and a vertical goniometer. The scanned angle interval was  $4^\circ < 2\theta < 70^\circ$  and the  $2\theta$  advance was  $0.02^\circ/\text{step}$  with a time interval of 3 s per step.

**Table 1** Quantitative elemental analysis (%mass) by EDFRX of the samples MHN08 and MHN09 from the Natural History Museum-UNMSM

Elements	Samples Concentration (%mass)	
	MHN 08	MHN 09
Si	25.34	48.09
K	0.13	0.10
Ca	0.10	0.10
Ti	0.03	0.04
V	0.00	0.00
Cr	0.06	0.07
Mn	0.07	0.08
Fe	9.11	9.45
Ni	0.00	0.05
Cu	0.003	0.01
Zn	0.01	0.04
As	—	0.05
Rb	0.02	0.03
Sr	—	0.004
La	0.20	0.20
W	—	0.11
Subtotal	35.073	58.424
Other (Z < 14)	64.927	41.576
Total %	100.00	100.00

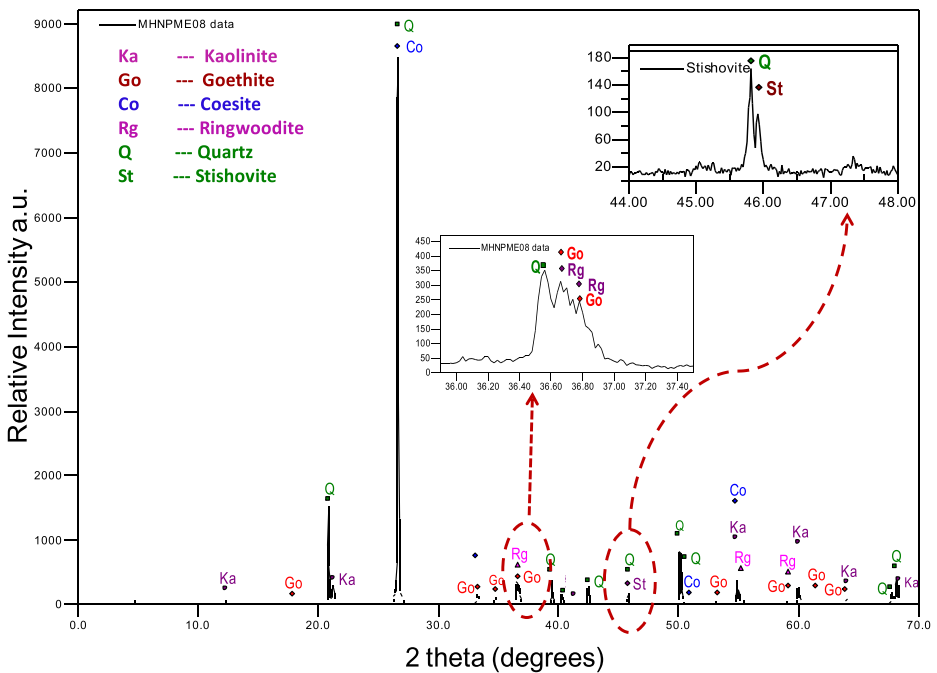


**Fig. 3** X-ray diffractogram of sample MHN-08

### 2.3 Analysis by $^{57}\text{Fe}$ transmission Mössbauer spectroscopy (TMS)

TMS was used to obtain more detailed information about iron containing minerals. A conventional spectrometer was used with a sinusoidal velocity modulation signal and 1024 channels for spectrum data storage. The Mössbauer spectrum at room temperature (RT:  $\approx 293$  K) was collected at the Laboratory of Archaeometry, Facultad de Ciencias Físicas, UNMSM. TMS measurements at LHT ( $\approx 4.2$  K) were collected at the Laboratoire de Centro Brasileiro de Pesquisas Físicas, CBPF, Brasil. A  $^{57}\text{Co}$  source in a Rh matrix was used to collect the spectra, which were analyzed and fitted using the NORMOS program (Brand, 1995) in its site and distribution versions, written by R. Brand [7].

### 3 Results and discussion

The results by the EDFRX technique allowed the determination of the quantitative elemental composition of the samples MHN-08 y MHN-09. Their spectra were collected under the following conditions:

**Sample MHN-08.** The X-ray source operated at 30.0 keV and 10.1  $\mu\text{A}$  which allowed a counting rate of 1400 cts/s.

**Sample MHN-09.** The X-ray source operated at 29.6 keV and 15.1  $\mu\text{A}$  which allowed a counting rate of 1532 cts/s.

It is observed that both samples have similar element concentrations for Ca, K, and Fe. The iron content is about 9%. It is in the content of Si where a large difference is found: Si (MHN-09) > Si (MHN-08).

Figure 3 shows the results by XRD. It shows the main peaks of the mineral phases of ringwoodite (Rw),  $(\text{Mg,Fe})_2\text{SiO}_4$ , which is a polymorph of olivine at high pressures; caolinite (Ca),  $\text{Al}_2(\text{Si}_2\text{O}_5)(\text{OH})_4$ ; quartz (Q),  $\text{SiO}_2$ ; goethite (Go),  $\text{Fe}^{3+}\text{O}(\text{OH})$ ; coesite (Co),  $\text{SiO}_2$ ; and stishovite (St),  $\text{SiO}_2$ . Overlapped peaks of Go+Co at  $2\theta = 33.24^\circ$ ; Go+Rw at  $2\theta = 36.64^\circ$  and  $59.03^\circ$ , are observed; quartz can be identified by its main peaks at  $2\theta = 20.89^\circ$ ;  $26.65^\circ$ ;  $50.12^\circ$  and  $68.12^\circ$ . Likewise, the most intense peak belongs to overlapped peaks of two phases, Co + Q at  $2\theta = 26.65^\circ$ . More overlapped peaks are observed for Q + Co; Co + St at  $2\theta = 40.0^\circ$  and for Q + St at  $2\theta = 45.9^\circ$ .

The results for sample MHN-09 are shown in Fig. 4, where the following structural phases are shown: goethite (Go), quartz (Q), coesite (Co), stishovite (St), ringwoodite (Rw), forsterite (Fo) ( $\text{Mg}_2\text{SiO}_4$ ) and wadsleyite (Wd),  $(\text{Mg, Fe}^{2+})_2\text{SiO}_4$ . Go is identified by its main peaks with highest intensities, which overlap: Go+Wd + Co at  $2\theta = 33.21^\circ$  and Go+Wd + Rw + Q at  $2\theta = 36.59^\circ$ , and the Go+Fo peaks overlap only at  $2\theta = 53.23^\circ$ , same as for Go+Rw which overlap at  $2\theta = 59.06^\circ$ . In all the cases when structural peaks of Go overlap with peaks of other phases, wide peaks are observed; this effect may be due to Go. Rw, a polymorph of olivine, and forsterite are present with their main peaks; their other peaks appear with low intensity. The overlapped peaks of Fo + Q are observed at  $2\theta = 39.50^\circ$ ; and at  $2\theta = 45.77^\circ$  are found the overlapped peaks of St + Q. Only two polymorphs of olivine are observed in this sample, Fo and Wd, which are produced by a transformation induced by the impact; there is overlap of several other peaks with Wd participating more.

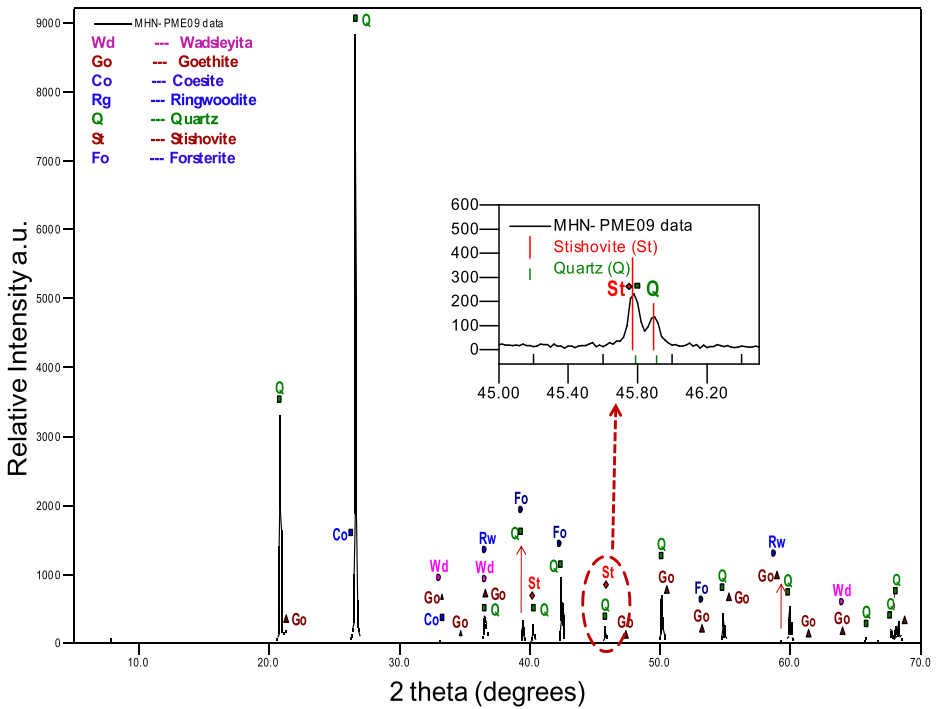


Fig. 4 X-ray diffractogram of sample MHN-09

Figures 5 (a) and (b) show the results by TMS of the sample MHN-08 taken at RT and LHT respectively. The spectra were fitted using the program NORMOS Brand using the Site and Dist versions. The analysis of the RT spectrum fitted with the Dist version shows three subspectra, two of them assigned to magnetic sextets and a doublet D1 assigned to a superparamagnetic  $\text{Fe}^{2+}$  site. One sextet S1, was fitted with an average magnetic field of  $\langle B_{\text{hf}} \rangle = 31$  T, assigned to Go; the second sextet S2, shows an average field of  $\langle B_{\text{hf}} \rangle = 20$  T.

The results obtained at THL were fitted with the Site version and show three sextets. Two of these sextets are related to the ones observed at RT but with higher magnetic fields; the third sextet is related to the doublet D1 which now appears magnetically ordered with a field of  $B_{\text{hf}} = 51.6$  T. The subspectrum S1 at RT shows a very broad area (80.8%); it may have occurred that due to the powerful meteoritic impact the soil grains might have suffered a grinding process that reduced their size that manifests itself at RT as with a strong superparamagnetic effect; after decreasing the temperature to liquid helium temperature, appears magnetically ordered.

Figure 6(a) shows the spectrum of the sample MHN-09 taken at RT which was fitted using the Dist version; it yielded three subspectra, two of which were assigned to the magnetic sextets S1 and S2, and the third one is assigned to a superparamagnetic doublet. The sextet S1 was assigned to the oxyhydroxide Go with an average field of  $\langle B_{\text{hf}} \rangle = 32$  T; the second sextet S2 has a field of  $\langle B_{\text{hf}} \rangle = 19$  T; and the doublet was assigned to an  $\text{Fe}^{2+}$  site, which can be assigned to the different silicate minerals found by XRD such as Forsterite, Wadsleyite and/or Ringwoodite,

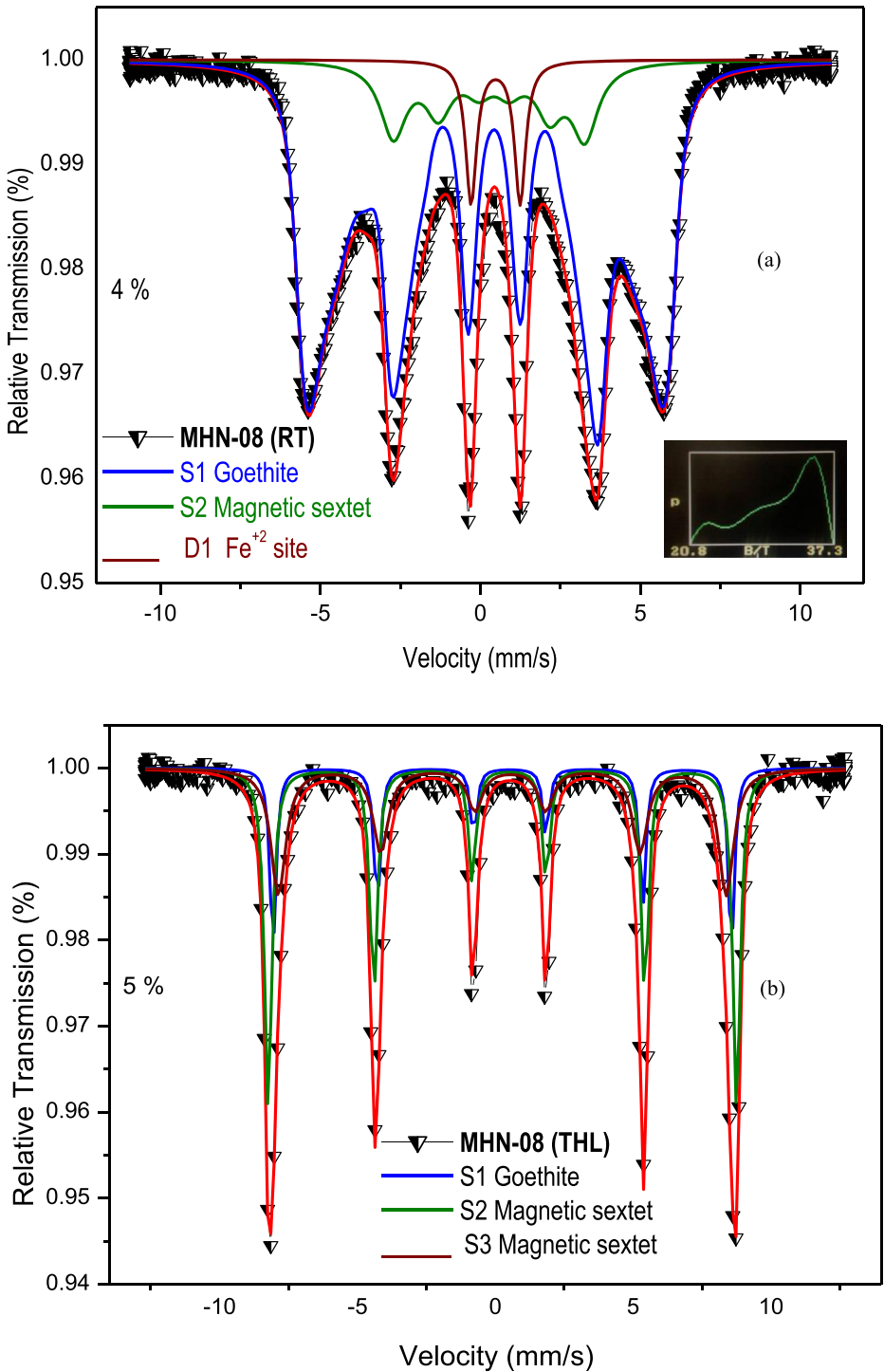


Fig. 5 Mössbauer spectrum of sample MHN-08 taken at different temperatures: (a) RT and (b) LHT

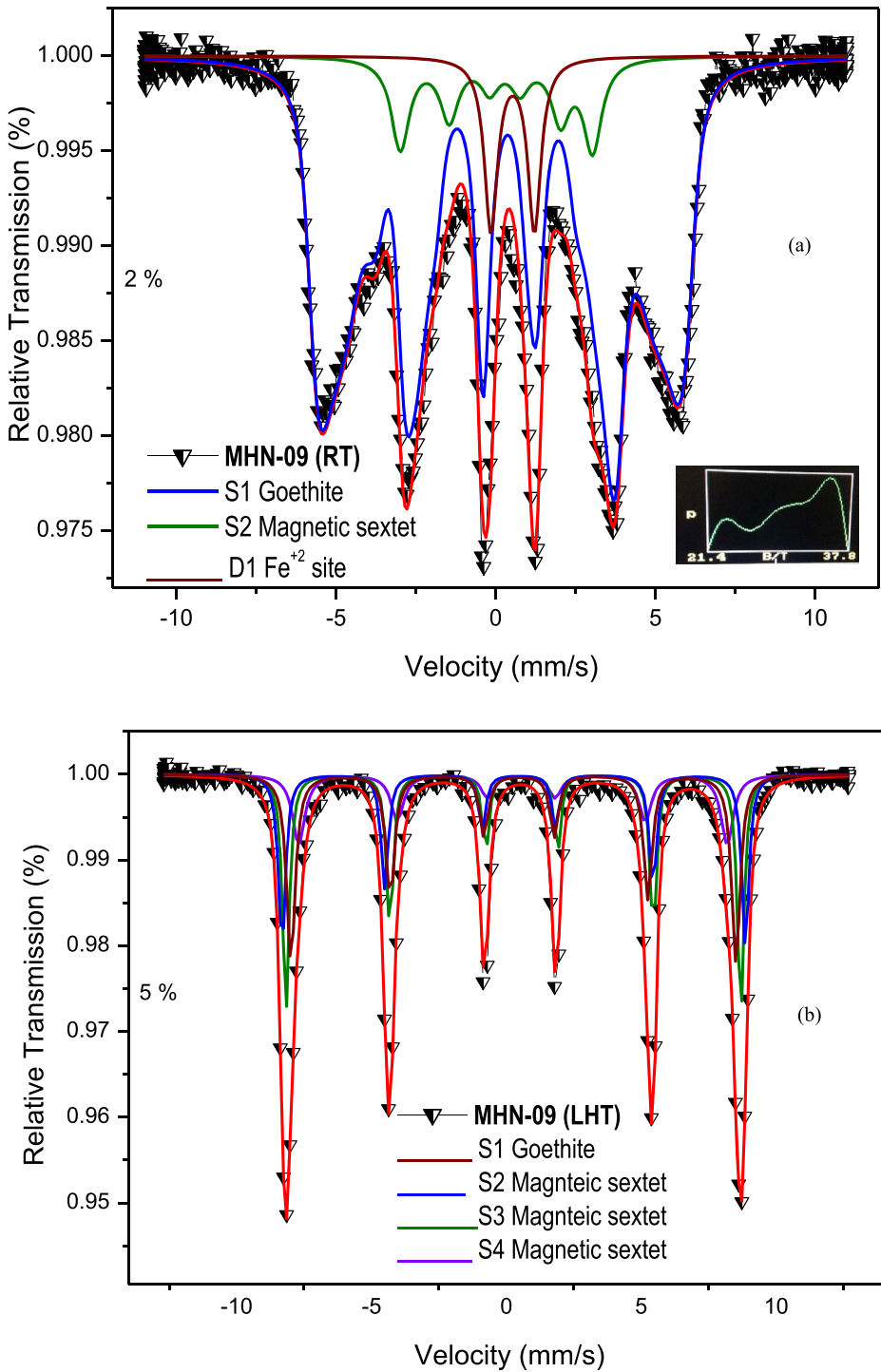


Fig. 6 Mössbauer spectrum of sample MHN-09 taken at different temperatures: (a) RT and (b) LHT



**Table 2** Hyperfine parameters of the Natural History Museum -UNMSM samples at RT

Natural History Museum Samples			
Room Temperature Measurements			
Sites	Parameters	MHN-08	MHN-09
Sextet S1/Go_Dist	$\delta$ (mm/s)	0.36(1)	0.29 (1)
	$2\varepsilon/\Delta E_Q$ (mm/s)	-0.27(1)	-0.30(1)
	$\langle B_{hf} \rangle$ (T)	31.0(1)	32.0(2)
	A (%)	80.8	82.46
	$\Gamma$ (mm/s)	0.52	0.49
Sexteto S2	$\delta$ (mm/s)	0.31(2)	0.02(4)
	$2\varepsilon/\Delta E_Q$ (mm/s)	-0.42(1)	-0.71(7)
	$B_{hf}$ (T)	20.0(2)	19.0(4)
	A (%)	13.62	10.49
	$\Gamma$ (mm/s)	0.99	0.69
D1 $Fe^{2+}$	$\delta$ (mm/s)	0.35(3)	0.39(3)
	$\Delta E_Q$ (mm/s)	1.53(1)	1.41(1)
	A (%)	5.6	7.06
	$\Gamma$ (mm/s)	0.42	0.50

**Table 3** Hyperfine parameters of the Natural history Museum- UNMSM sample at LHT

Natural History Museum Samples			
Measurements at LHT			
Sites	Parameters	MHN-08	MHN-09
Sextet S1 Goethite	$\delta$ (mm/s)	0.37(3)	0.40(4)
	$2\varepsilon/\Delta E_Q$ (mm/s)	-0.23(2)	-0.23(2)
	$B_{hf}$ (T)	53.0(3)	52.3(2)
	A (%)	43	30
	$\Gamma$ (mm/s)	0.33	0.40
Sextet S2 Goethite	$\delta$ (mm/s)	0.44(2)	0.36(1)
	$2\varepsilon/\Delta E_Q$ (mm/s)	-0.30(2)	-0.19(1)
	$B_{hf}$ (T)	52.0(2)	51.0(6)
	A (%)	21.0	31
	$\Gamma$ (mm/s)	0.27	0.38
Sextet S3	$\delta$ (mm/s)	0.42(2)	0.40(1)
	$2\varepsilon/\Delta E_Q$ (mm/s)	-0.29(2)	-0.31(1)
	$B_{hf}$ (T)	51.6(1)	53.4(3)
	A (%)	35	16.40
Sextet S4	$\Gamma$ (mm/s)	0.67	0.55
	$\delta$ (mm/s)		0.37(3)
	$2\varepsilon/\Delta E_Q$ (mm/s)		-0.18(2)
	$B_{hf}$ (T)		49.3(3)
	A (%)		23.29
	$\Gamma$ (mm/s)		0.26

which according to their elemental composition contain Mg and  $Fe^{2+}$ . The spectrum taken at LHT was fitted using the SITE version as is shown in Fig. 6(b) and shows four subspectra: two sextets S1 and S2, with relative areas of 30% and 31% respectively, which are assigned to Go; sextet S3 (with  $\langle B_{hf} \rangle = 19$  T at RT), now

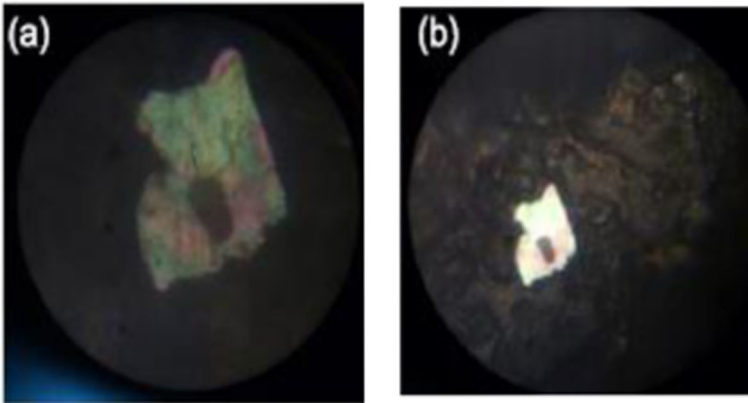


**Fig. 7** Sample MHN.08, with magnification of (a) 400 X and (b) 100 X

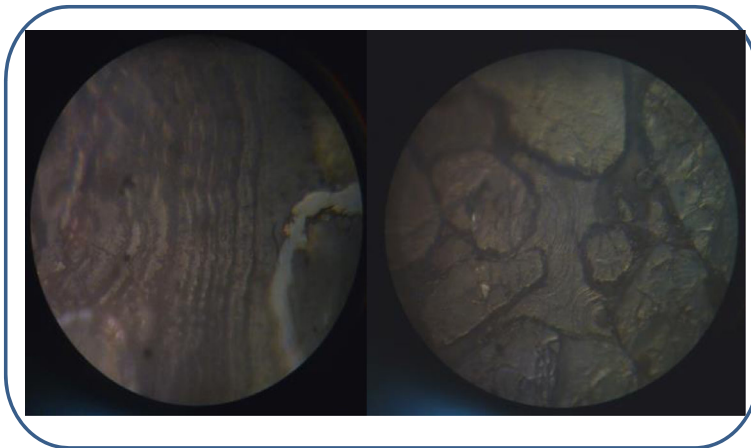


**Fig. 8** MHN-09 taken with a MOM at 100X (left), where gaps and grooves are generated by the impact; and at 400X (right), it shows the eudral shape of the sample

at LHT with a magnetic field of  $B_{hf} = 53.4$  T; and the doublet D1 at RT now at LHT appears magnetically ordered, sextets S4, with a field of  $B_{hf} = 49.3$  T.

The recorded hyperfine parameters of the samples MHN-08 and MHN-09 at RT and LHT, were results of the comparative analysis with the parameters published in the Mössbauer Minerals Handbook [8] and are listed in the Tables 2 and 3.

### 3.1 Analysis by metallographic optical microscopy (MOM)

#### 3.1.1 Sample MHN-08

Fig. 7a and b show the points that were analyzed by MOM with magnification of 400 X and 100 X respectively.

### 3.1.2 Sample MHN-09

The results can be observed in the Fig. 8 which show clearly the eudral forms of the sample that were observed with the MOM at a scale of 100X showing the presence of minerals such as quartz.

In both samples it is observed very clearly the presence of grooves and foldings in the samples that could be the result of a powerful collision with the surface with the generation of very intense pressure and high temperature in the soil.

## 4 Conclusions

The results obtained by the application of analytical techniques show the advantages for obtaining basic information about the studied samples. Moreover, other complementary technique such as MOM allowed to better define the morphological and pointwise characterization of each sample, classifying to the samples MHN-08 and MHN-09 areas impactites because of the presence of coesite, stishovite, and ringwoodite.  $^{57}\text{Fe}$  Mössbauer spectroscopy allows verifying that the main magnetic phase is due to the oxihydroxide of iron goethite.

**Acknowledgements** We acknowledge the contribution of Prof. Guillermo Morales Serrano who donated his collection of mineral samples to the MHN. We also acknowledge the contribution of the Laboratories of Analysis of Soils, Archaeometry, and X-Ray Diffractometry at San Marcos University, and of Mössbauer Spectroscopy at CBPF.

## References

1. Loayza, M.L.C., Cabrejos, J.A.B.: Minerals of a soil developed in the meteoritic crater of Carancas, Perú, and evidences of phase changes on the impact event. *Hyperfine Interact.* **224**, 143–152 (2014)
2. Loayza, M.L.C., Cabrejos, J.A.B.: Characterization of the Carancas-Puno meteorite by energy dispersive X-ray fluorescence, X-ray diffractometry and transmission Mossbauer spectroscopy. *Hyperfine Interact.* **203**, 17–23 (2011)
3. Cerón Loayza, M.L., Bravo Cabrejos, J.A.: Caracterización Mineralógica de un Impacto Meteorítico en la Localidad de Carancas–Puno. *Rev. Investig. Fis.* **12**(1), 5–12 (2009).
4. Wackerle, J.: Shock-wave compression of quartz. *J. Appl. Phys.* **33**, 922–937 (1962)
5. Kieffer, S.W., Phakey, P.P., Christie, J.M.: *Contrib. Mineral. Petrol.* **1**(59), 41–93 (1976)
6. Holland, K.G., Ahrens, T.J.: Melting of  $(\text{mg,Fe})_2\text{SiO}_4$  at the core-mantle boundary of the earth. *Science*. **275**, 1623–1625 (1997)
7. Brand, R.A.: Normos-90 Mössbauer Fitting Program Package. U. of Duisburg, Alemania (1994)
8. Stevens, J. (ed.): *Mössbauer Minerals Handbook*, Mössbauer Effect Data Center. Ashville (1998)

**Publisher's note** Springer Nature remains neutral with regard to jurisdictional claims in published maps and institutional affiliations.